Article

Not peer-reviewed version

Cold Dispase Digestion of Murine Lungs Improves Recovery and Culture of Airway Epithelial Cells

Piotr P. Janas , Caroline Chauché , Patrick Shearer , Georgia Perona-Wright , Henry J. McSorley , Jürgen Schwarze *

Posted Date: 12 July 2023

doi: 10.20944/preprints202307.0769.v1

Keywords: airway epithelial cells; cell culture; MACS; dispase; cold lung digestion

Article

Cold Dispase Digestion of Murine Lungs Improves Recovery and Culture of Airway Epithelial Cells

Piotr P Janas[1], Caroline Chauché[1], Patrick Shearer[2], Georgia Perona-Wright[2], Henry J McSorley[3] and Jürgen Schwarze[1*]

[1] Centre for Inflammation Research, Institute for Regeneration and Repair, The University of Edinburgh, Edinburgh BioQuarter, Edinburgh, EH16 4UU, United Kingdom
[2] Institute of Infection, Immunity & Inflammation, University of Glasgow, Glasgow, G12 8TA, United Kingdom
[3] Division of Cell Signalling and Immunology, School of Life Sciences, University of Dundee, Dundee, DD1 5AA, United Kingdom
* Correspondence: Jurgen.Schwarze@ed.ac.uk

Abstract: Airway epithelial cells (AECs) play a key role in maintaining lung homeostasis, epithelium regeneration and the initiation of pulmonary immune responses. To isolate and study murine AECs investigators have classically used short and hot (1h 37°C) digestion protocols. Here, we present a workflow for efficient AECs isolation and culture, utilizing long and cold (20h 4°C) dispase II digestion of murine lungs. This protocol yields a greater number of viable AECs compared to an established 1h 37°C dispase II digestion. Using a combination of flow cytometry and immunofluorescent microscopy, we demonstrate that compared to the established method, the cold digestion allows for recovery of a 3-fold higher number of $CD45^{-}CD31^{-}EpCAM^{+}$ cells from murine lungs. Their viability is increased compared to established protocols, they can be isolated in larger numbers by magnetic-activated cell sorting (MACS), and they result in greater numbers of $KRT5^{+}p63^{+}$ colonies *in vitro*. Our findings demonstrate that temperature and duration of murine lung enzymatic digestion have a considerable impact on AEC yield, viability, and ability to form colonies *in vitro*. We believe this workflow will be helpful for studying lung AECs and their role in the biology of lung.

Keywords: airway epithelial cells; cell culture; MACS; dispase; cold lung digestion

1. Introduction

The airway epithelium forms an important barrier at the interface of environment and organism [1]. AECs consist of heterogenous groups of cells, including pneumocytes, goblet, club, ciliated and basal cells [2,3]. Depending on the species and anatomic location in the airways, different proportions of AEC subsets have been observed. The epithelium of large airways in humans forms a pseudostratified layer with ciliated, goblet and club cells at the luminal side, while underlying basal cells are attached to the basement membrane. On the other hand, the pseudostratified epithelium in mice is limited to the trachea, with simpler columnar epithelium present in the bronchi [1]. It is thought that in mice the majority of airway basal cells are limited to the trachea, with sparse basal cells in bronchi [1]. Among AECs, basal cells keep the greatest degree of pluripotency allowing them to proliferate and differentiate into various subtypes of epithelial cells. Thus, basal cells play a major role in airway epithelium homeostasis and repair [2,3] and they are also essential for *in vitro* primary AECs cultures since they can be maintained in a constant proliferative state [4–6].

Isolated primary AECs are used in a range of *in vitro* experimental systems. Most commonly, when maintained in media containing differentiation inhibitors, primary AECs can be sub-cultured in a monolayer. However, when cultured in well-plate inserts with specialised media, air-liquid interface (ALI) cultures can be established [4]. ALI cultures recapitulate the epithelium of large airways as these cultures are pseudostratified and AECs differentiate into various subsets including ciliated, club or goblet cells. ALI cultures also exhibit mucociliary motion, produce mucus and develop tight junctions [7–9]. Subsets of AECs can also be cultured in a Matrigel matrix to generate tracheospheres, bronchiolospheres or alveolospheres [10,11]. All these experimental systems can be

 doi:10.20944/preprints202307.0769.v1

used to study AEC biology at homeostasis, after injury e.g. by respiratory pathogens, and during regeneration.

In recent years, it has been recognised that AECs do not only form an inert barrier, but that they are a dynamic and versatile cell population that is involved in maintaining lung homeostasis [12], mounting initial immune responses [13] and lung regeneration following injury [14]. The manifold roles of AECs implicate them in pathogenesis of a number of diseases ranging from asthma [15], COPD [16] to lung fibrosis [17]. An increasing number of research questions focusing on AECs in various contexts creates a demand for improved and well-defined methodologies allowing for their efficient harvest, isolation and culture.

In order to study primary AECs *in vitro*, various digestion techniques have been employed that allow for disruption of cell junctions and connective tissue resulting in lung single cell suspension. To isolate and study AECs from a murine lung, researchers commonly utilize a combination of dispase II and DNase I enzymes at 37°C for 30-60min [18–20] (hot digestion). However, when we employed this established digestion method, we found that the yield and viability of AECs was unsatisfactory in the context of MACS sorting and *in vitro* culture. We therefore investigated alternative workflows. While there are several digestion methods for murine lungs utilizing a range of enzymes including collagenases, dispases, liberase, pronase and trypsin [21], we investigated the effects of digestion time and temperature rather than the type of enzyme. It has been shown that long, overnight digestion can be beneficial to yield and efficiency when isolating cells from human skin [22], or human brain tissue [23]. Following on from a method where murine tracheas were digested for 18h at 4°C using pronase [24], we assessed a 20h 4°C dispase II/DNase I digestion of murine lungs (cold digestion).

Here, we present a workflow that in comparison to the commonly used hot dispase digestion allows for retrieval of a 3-fold higher number of $CD45^-CD31^-EpCAM^+$ AECs with a higher proportion of viable cells. This in turn allows for recovery of greater numbers of AECs after MACS sorting and a greater yield of keratin 5 $(KRT5)^+$ $p63^+$ basal cell colonies *in vitro* after seven-day culture.

2. Materials and Methods

2.1 Animals

C57BL/6 mice were bred and housed at the University of Edinburgh. All procedures approved by the University of Edinburgh Animal Welfare and Ethical Review Board, and performed under UK Home Office licenses with institutional oversight performed by qualified veterinarians. UK Home Office project license to JS, number P4871232F. ARRIVE guidelines were followed.

2.2 Murine Lung Harvest and Digestion

Adult C57BL/6 mice over six weeks of age were anaesthetized with a 1:1 mixture of ketamine and medetomidine through intraperitoneal (IP) injection with a dose dependent on the body weight. Mice were then terminally exsanguinated, and death confirmed by cervical dislocation. The abdominal aorta was cut, and the trachea exposed by removing the salivary glands. The trachea was then cannulated using a blunt needle and bronchoalveolar lavage with ice-cold Dulbecco's Modified Eagle Medium/Nutrient Mixture F-12 (DMEM/F12) (Gibco) was performed (0.8ml per mouse). The rib cage was then removed, and cardiovascular system was flushed by injecting 10ml of ice-cold DMEM/F12 into the right ventricle. A volume of 1.5-2ml of enzyme mix was then slowly injected through the tracheal cannula into the lungs, which were then removed (lungs were dissected out of the thoracic cavity by cutting at the primary bronchial bifurcation) and placed in 3ml of digestion mixture (2mg/ml Dispase II (Sigma-Aldrich) + 0.1mg/ml DNaseI (Sigma-Aldrich) re-suspended in DMEM/F12 (Gibco) + 1% v/v Penicillin-Streptomycin (Gibco)). The digestion mixture was previously filtered through 0.22µm filter and frozen. Lungs were then incubated for 1h at 37°C or 20h at 4°C. The digestion solution together with lungs was then poured onto a 70µm strainer, lungs were then dissociated using a 5ml syringe plunger by gently agitating the lungs on the mesh. The strainer was then washed using 10ml of dispase wash (DMEM/F12 (Gibco) + 0.05mg/ml DNaseI (Sigma-Aldrich) + 1% v/v Penicillin-Streptomycin (Gibco)). Each sample was then centrifuged for 15min, 4°C, 130 relative centrifugal force (RCF). The supernatant was then removed and 2ml of ice-cold ACK red blood cell lysis (Gibco) was added to each tube, samples were swirled for 90s, and 5ml of MACS buffer (Phosphate-buffered saline (PBS) - no Mg^{2+} and Ca^{2+} + 0.5% bovine serum albumin (BSA) + 2mM ethylenediaminetetraacetic acid (EDTA)) was added. Samples were then passed through a

 doi:10.20944/preprints202307.0769.v1

40µm strainer, washed with 5ml of MACS buffer and centrifuged for 5min, 4°C at 300 RCF. Each sample was then resuspended in 1ml of MACS buffer and blocked with 5µl of 0.5mg/ml anti-mouse CD16/32 antibody (BioLegend) ready for further MACS processing or flow cytometry staining.

2.3 Airway Epithelial Cell Sorting (MACS)

After incubation cells were centrifuged for 5min, 4°C, 300 RCF and resuspended in 85µl of MACS buffer + 5µl of anti-CD31 microbeads and 10µl of anti-CD45 microbeads (Miltenyi Biotec) per 10^7 total cells. Samples were then incubated for 30 minutes on ice. Each sample was then washed with 1ml/10^7 cells of MACS buffer and centrifuged for 5min, 4°C at 300 RCF. Cells were then passed through LS MACS columns (Miltenyi Biotec) on a QuadroMACS separator (Miltenyi Biotec) and flow-through was collected. Collected cells were then centrifuged for 5min, 4°C, 300 RCF and resuspended in leftover liquid, and 15µl of anti-EpCAM microbeads (Miltenyi Biotec) was added. Samples were incubated on ice for 30 minutes, washed with 1ml MACS buffer, and centrifuged for 5min, 4°C, 300 RCF. Supernatant was discarded, and cells were resuspended in 500µl of MACS buffer. The cell suspension was then passed through a MS MACS column using an OctoMACS separator (Miltenyi Biotec). EpCAM+ cells were then gently flushed out of the column by applying 2ml of MACS buffer and inserting the plunger into the column. Cells were then centrifuged for 5min at 4°C, 300 RCF, supernatant was removed, and the cell pellet was resuspended in 0.5ml of MACS buffer. 10µl of cell suspension was then aspirated and gently mixed with 10µl of 0.1% trypan blue (Gibco) by pipetting up and down. Immediately afterwards, 10µl of cell suspension was placed in Neubauer improved counting chamber (haemocytometer) and covered with coverslip. Cells were then manually counted and total amount of live (trypan blue negative) and dead (trypan blue positive) cells in suspension was calculated.

2.4 Primary AECs In Vitro Culture

24-well plates were coated with a coating solution that combines 30µg/ml of type I calf skin collagen (Sigma-Aldrich), 10µg/ml human placental fibronectin (Bio-Techne) and 10µg/ml bovine serum albumin (BSA – Sigma-Aldrich) in HBS (Gibco), for at least 4-8h at 37°C. A total of $2x10^5$ MACS sorted AECs were seeded per well and 0.5ml media was changed after 24h, and then every two days thereafter. Media was prepared by combining supplemented PromoCell Epithelial Growth Medium with 1µM A3801 (STEMCELL Technologies) and 0.2µM DMH-1 (STEMCELL Technologies) SMAD signalling inhibitors, 5µM Y27632 ROCK (STEMCELL Technologies) pathway inhibitor, 0.5µM CHIR9902 (STEMCELL Technologies) WNT pathway activator and 1% v/v Penicillin/Streptomycin (Gibco). Cells were cultured for seven days, followed by immunofluorescent microscopy of each well.

2.5 Immunofluorescent Microscopy

Cells in each well were washed with PBS three times and fixed using 4% PFA solution for 10min at room temperature (RT). Fixed cells were then stored in 70% Ethanol at 4°C until staining. Cells were permeabilised with a 1% BSA and 0.2% triton X-100 (Sigma-Aldrich) solution at RT for 10min. Cells were then blocked for 45min at RT using a 5% goat serum, 1% BSA and 0.1% Tween-20 (Sigma-Aldrich) in PBS. Cells were then stained with a mix of primary antibodies (anti-KRT5, anti-p63 and anti-E-Cadherin-eF660), overnight at 4°C, followed by three washes with blocking buffer (each wash for 5min) and staining with secondary antibodies (anti-rabbit-AF488, anti-mouse-AF555) as well as 1:500 10mg/ml Hoechst (Invitrogen) for nuclear counter stain for 1h at RT. Secondary antibodies were then washed away with three washes (each wash for 5min) with blocking buffer followed by filling each well with 0.7ml PBS.

Imaging was performed using EVOS FL Auto 2 (Thermo Fisher Scientific), using 20x objective as well as DAPI, GFP and RFP light cubes. Scans were set to a custom calibrated Corning 24-well plate, where 25% of each well was scanned from the middle using the "more overlap" setting and manually set focus for each channel. Images were analysed using ImageJ, with ICA LUT (look-up table) set for KRT5 for easier basal AECs identification. All micrograph related colony counting was performed while blinded.

Surface area of KRT5 colonies was calculated using ImageJ. At first KRT5 images were converted to 8-bit. Then images were smoothed out using median filter (7px value), followed by thresholding using "mean setting". Images were then converted to binary format and surface area of black pixels was calculated using "Analyze particles" tool. Obtained pixel numbers were then converted to total surface in mm^2 based on image metadata (scale).

Preprints (www.preprints.org) | NOT PEER-REVIEWED | Posted: 12 July 2023 doi:10.20944/preprints202307.0769.v1

Table 1. List of microscopy antibodies.

Antibody name	Supplier	Host species	Antibody type	Clone	Catalogue number	Dilution
Anti-p63	Abcam	Mouse	Monoclonal	4A4	ab735	1:200
Anti-KRT5	BioLegend	Rabbit	Polyclonal	Poly19055	905503	1:500
Anti-E-cadherin (CD324) eFluor 660	Thermo Fisher Scientific	Rat	Monoclonal	DECMA-1	50-3249-82	1:30
Rat IgG1 kappa Isotype Control (eBRG1) eFluor 660	Thermo Fisher Scientific	Rat	Isotype control	eBRG1	50-4301-82	1:30
Goat Anti-Rabbit IgG (H+L) Alexa Fluor 488	Thermo Fisher Scientific	Goat	Polyclonal, secondary	Reactivity - rabbit	A-11008	1:200
Goat Anti-Mouse IgG (H&L) Alexa Fluor 555	Abcam	Goat	Polyclonal - secondary	Reactivity - mouse	ab150114	1:200

2.6 Flow Cytometry

Following digestion, numbers of cells in each sample were calculated using a haemocytometer. $0.5x10^6$ total cells from each sample were then washed twice with PBS and stained using a LIVE/DEAD fixable near-IR stain (Invitrogen) in PBS for 30min on ice, followed by two washes with PBS and staining with a combination of anti-CD45, anti-CD31 and anti-EpCAM in PBS + 1% BSA for 30min on ice. Stained samples were then washed twice with PBS + 1% BSA. Whole samples were acquired and unmixed using Cytek Aurora with Cytek SpectroFlo 3.0.3 and analysed using De Novo Software FCSexpress 7.

The gating strategy involved debris exclusion (side scatter/forward scatter – SSC-H/FSC-H), followed by selection for singlets (FSC-H/FSC-A) and dead cell exclusion (LIVE/DEAD Fixable Near IR/FSC-H). Dead cell exclusion was performed at the end of gating strategy for viability evaluation in Figure 2b. Leukocytes and endothelial cells were then excluded using CD45/CD31 gate, followed by selection for AECs with EpCAM/SSC-H gate.

Table 2. List of flow cytometry antibodies.

Antibody name	Supplier	Host species	Antibody type	Clone	Catalogue number	Dilution
Anti-CD45 Pacific Blue	BioLegend	Rat	Monoclonal	S18009F	157212	1:200
Anti-CD45 AF700	BioLegend	Rat	Monoclonal	S18009F	157210	1:200
Anti-CD31 BV605	BioLegend	Rat	Monoclonal	390	102427	1:600
Anti-CD31 BV421	BioLegend	Rat	Monoclonal	390	102423	1:300
Anti-EpCAM PE/Dazzle594	BioLegend	Rat	Monoclonal	G8.8	118236	1:300
Anti-EpCAM BV605	BioLegend	Rat	Monoclonal	G8.8	118227	1:300
Anti-CD24 PE/Cyanine7	BioLegend	Rat	Monoclonal	M1/69	101821	1:200

Preprints (www.preprints.org) | NOT PEER-REVIEWED | Posted: 12 July 2023 doi:10.20944/preprints202307.0769.v1

Anti-CD49f BV605	BioLegend	Rat	Monoclonal	GoH3	313625	1:100

2.7 RNA Isolation and qPCR (Quantitative Polymerase Chain Reaction)

After CD45-CD31-EpCAM+ MACS sorting cells were centrifuged for 5min, 4°C, 300 RCF and resuspended in 0.5ml of TRizol. Following 5min incubation at RT, samples were stored at -80°C before further processing. Samples were then thawed and 100ul of bromochloropropane (Sigma-Aldrich) was added per 500ul of TRizol. Samples were shaken vigorously for 30s until they acquired a milky-pink shade. Samples were then incubated at RT for 10min, and then cooled down on ice for 5min before centrifugation at 4°C, 16,000 RCF for 20min. 200µl of the top aqueous phase was then transferred to fresh Eppendorf test tubes and 250µl of RNase-free isopropanol (Merck) and 1µl of GlycoBlue Coprecipitant (Invitrogen) were added. Test tubes were inverted ten times and incubated at RT for 10min, followed by centrifugation at 4°C, 16,000 RCF for 10min. Blue RNA pellet could now be observed at the bottom of test tubes. Supernatant was removed and pellet was washed three times using 1ml of RNase-free 75% EtOH (Merck), with 5min 4°C, 16,000 RCF centrifugations between each wash. After final wash, ethanol was discarded, and pellets were air-dried until no liquid could be seen in test tubes. Pellets were then resuspended in 30µl of RNAse-free water (QIAGEN), and amount of RNA was quantified using NanoDrop One/OneC Microvolume UV-Vis Spectrophotometer (Thermo Scientific). The amount of RNA was normalised in each sample using RNase-free water and 300ng of RNA was converted to cDNA using High-Capacity cDNA Reverse Transcription Kit (Applied Biosystems). qPCRs were performed in duplicates using Fast SYBR Green Master Mix (Applied Biosystems) and StepOne (Thermo Fisher Scientific) thermocycler. 100nM of forward and reverse primers, as well as 10ng of cDNA, were added to each qPCR reaction. *Rpl37* was used as an endogenous control. Genomic DNA contamination was assessed by performing a qPCR reaction on non-reverse transcribed RNA sample.

Table 3. List of PCR primers.

Primer	Sequence
Ldha forward	CATTGTCAAGTACAGTCCACACT
Ldha reverse	TTCCAATTACTCGGTTTTTGGGA
Rpl37 forward	CCAAGCGCAAGAGGAAGTATAAC
Rpl37 reverse	GAATCCATGTCTGAATCTGCGG

2.8 Statistical Analysis

Data in the plots are represented as medians with boxes representing interquartile ranges and bars corresponding to minima and maxima. MFI is reported as median fluorescence intensity. Statistical differences were assessed using an unpaired two-tailed t-test. Data in the text is presented as means with standard error. All statistical analysis was performed using GraphPad Prism 8.4.3.

3. Results

3.1. Cold Digestion Provides Greater Yield and Viability of AECs Compared to Hot Digestion

We used flow cytometry (**Figure 1a**) to assess the yield of three different cell populations after a 1h 37°C dispase II/DNase I digestion of murine lungs. On average, we obtained 5.55 ± 0.05 x10^5 CD45$^-$CD31$^-$EpCAM$^+$ AECs (7% of total cells), 7.35 ± 0.59 x10^6 CD45$^+$ immune cells and 2.10 ± 0.03 x10^5 CD31$^+$ endothelial cells (**Figure 1b**).

We decided to investigate whether the use of cold digestion of murine lungs would increase the yield and/or viability of AECs. Using the cold digestion approach, the average number of isolated CD45$^-$CD31$^-$EpCAM$^+$ AECs increased to 1.46 ± 0.15 x10^6, almost 3-fold the number obtained following hot digestion. Likewise, the number of CD31$^+$ endothelial cells obtained with the cold digestion (4.27 ± 0.05 x10^5) was almost 2-fold higher than after hot digestion. Conversely, the number of CD45$^+$ cells was similar between the two digestion techniques. This suggests that the cold digestion approach is beneficial for recovery of structural cells from the lung, while obtaining similar numbers of lung immune cells.

While several cell surface markers like CD4, CD8 or PD-1L are known to be sensitive to dispase II digestion *[25]*, we did not find any changes in expression levels of CD45, CD31 and EpCAM between the digestion methods as seen by comparable MFI (median) levels of each marker irrespective of digestion method (**Figure 1c**). We also did not observe loss of several AECs-related cell

Preprints (www.preprints.org) | NOT PEER-REVIEWED | Posted: 12 July 2023 doi:10.20944/preprints202307.0769.v1

surface markers such as major histocompatibility (MHC) I, MHC-II or CD24 (Supplementary Figure 1).

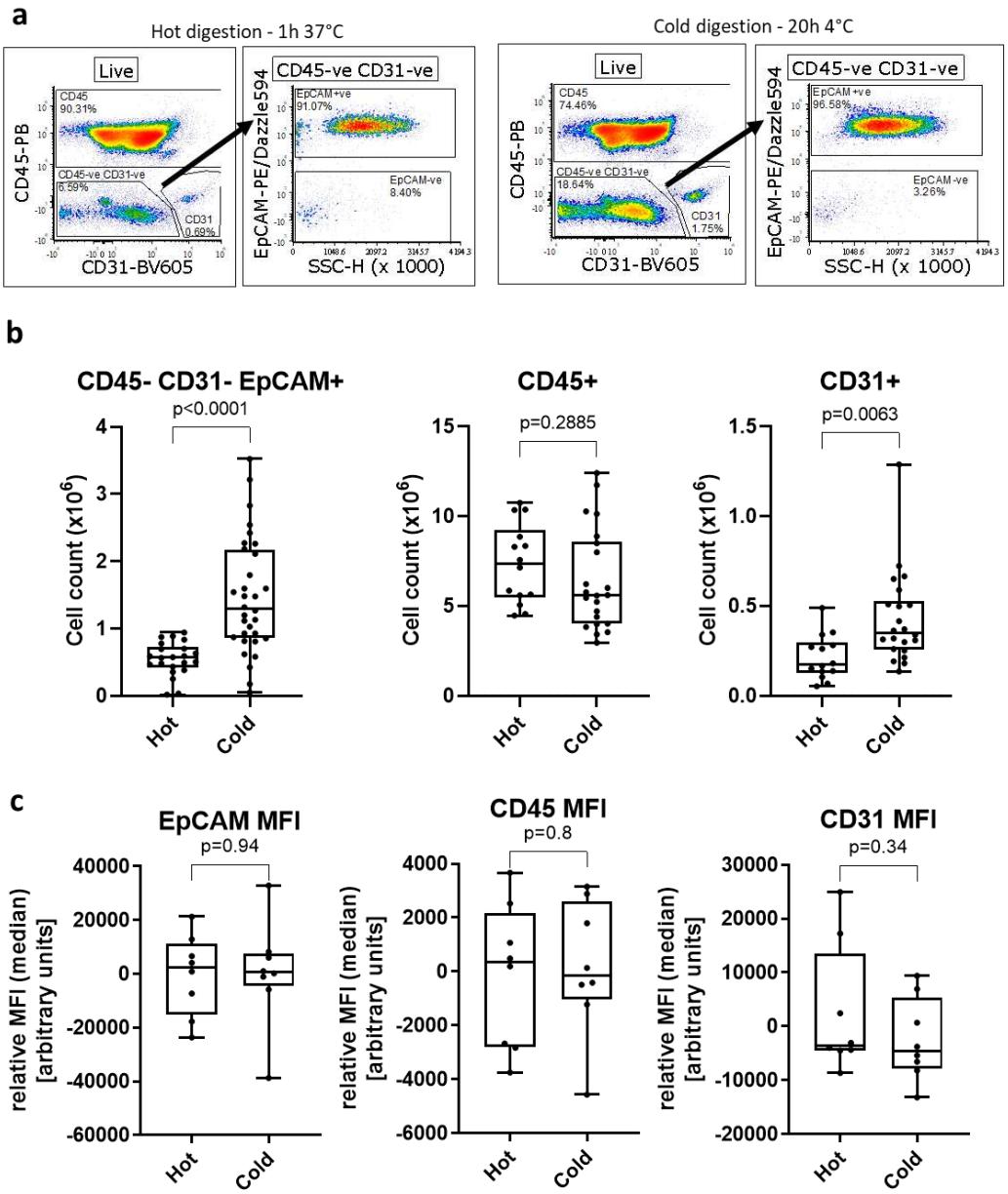

Figure 1. Flow cytometric analysis of murine lung digests with lung inflation, comparing the number of cells after hot (1h, 37°C) or cold (20h, 4°C) digests. (**a**) Representative gating strategy following debris exclusion (FSC/SSC), singlets (FSC-H/FSC-A) and dead cells exclusion (LIVE/DEAD fixable near-IR). CD45$^-$CD31$^-$ cells are gated, followed by EpCAM$^+$ve gating. (**b**) Number of CD45$^-$CD31$^-$ EpCAM$^+$ AECs, CD31$^+$ endothelial cells or CD45$^+$ leukocytes. (**c**) Comparison of relative MFI (median) values for EpCAM, CD45 and CD31 between cold and hot digests within respective CD45$^-$CD31$^-$ EpCAM$^+$, CD45$^+$ and CD31$^+$ gates. Each data point represents a lung from a single mouse. Unpaired t-test, median ± min/max

3.2. Following Cold Digestion, More AECs Are Viable Compared to Hot Digestion

Next, we compared the viability of isolated AECs between cold and hot lung digestions by flow cytometry, assessing the proportion of live cells within the CD45$^-$CD31$^-$EpCAM$^+$ population in single cell suspension, with the gating strategy shown in Figure 2a. We found that on average 83.99 ± 1.16% of CD45$^-$CD31$^-$EpCAM$^+$ cells from cold lung digestions were alive, compared to 56.65 ± 3.16% after hot digestion, a 1.48-fold increase in viable AECs (Figure 2b). Despite differences in viability of AECs,

Preprints (www.preprints.org) | NOT PEER-REVIEWED | Posted: 12 July 2023 doi:10.20944/preprints202307.0769.v1

we did not observe changes in levels of Ldha (a marker of oxidative stress) *[26]* between digestion methods (Supplementary Figure 2).

Given this increased viability, we hypothesised that MACS sorting, and subsequent seeding of AECs isolated by cold digestion would result in a greater number of basal AEC colonies in in vitro cultures, comparted to hot digestion. Performing double MACS sorting with initial CD45 and CD31 depletion followed by EpCAM positive selection, we recovered substantially more AECs following cold digestion (5.30 ± 0.45 x10^5 AECs) compared to hot digestion (2.97 ± 0.26 x10^5 AECs) which is equivalent to a 1.78-fold increase in number of viable AECs (Figure 2c). The AECs recovered after MACS sorting were highly pure (Figure 2d), with average purity of 96.35 ± 0.75% CD45$^-$CD31$^-$EpCAM$^+$ cells of live cells. To confirm the airway epithelial identity of sorted CD45$^-$CD31$^-$EpCAM$^+$ we used flow cytometry to confirm that these cells also express other epithelial markers. Virtually all CD45$^-$CD31$^-$EpCAM$^+$ cells also expressed CD49f (integrin α6) *[27,28]* and CD24 *[29,30]* (Figure 2e), albeit as expected, at vastly varying levels.

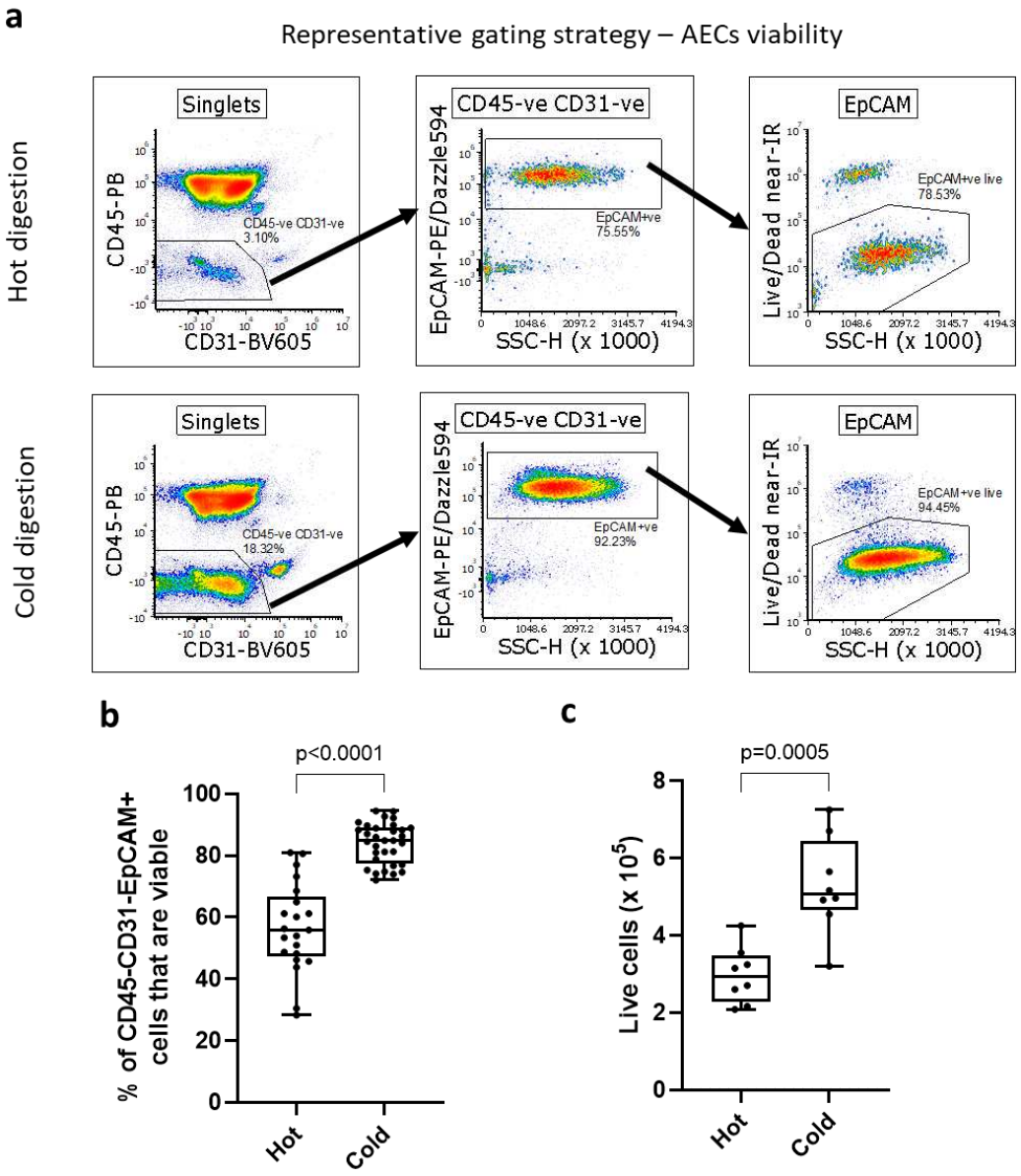

Preprints (www.preprints.org) | NOT PEER-REVIEWED | Posted: 12 July 2023 doi:10.20944/preprints202307.0769.v1

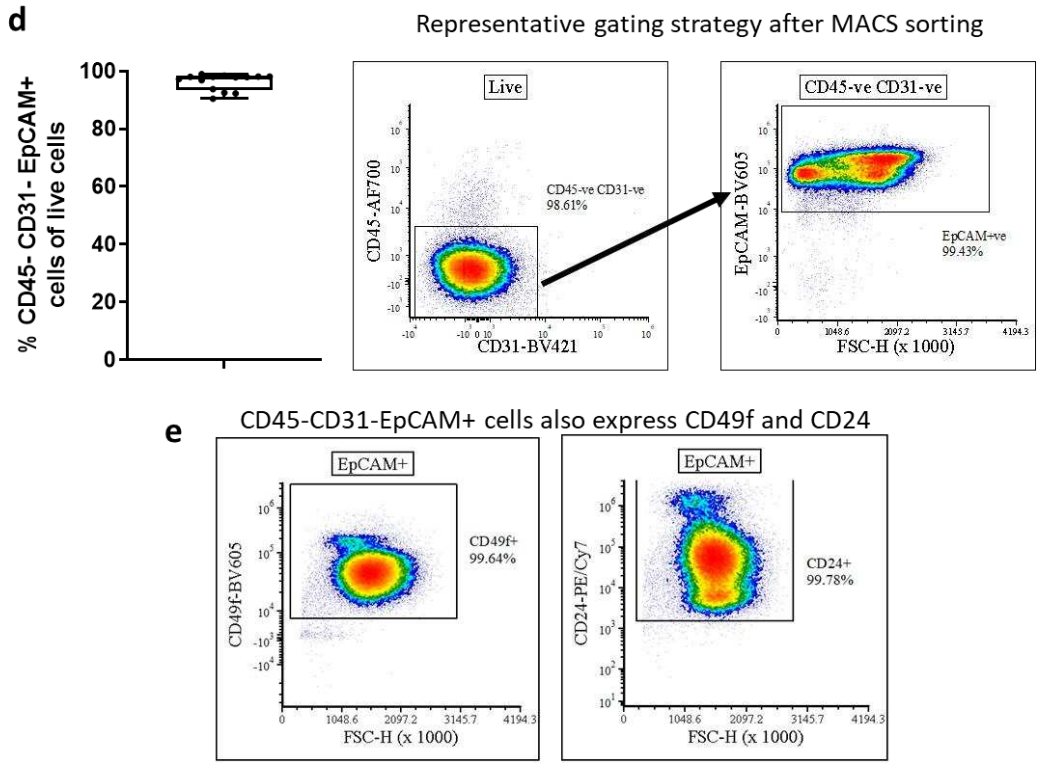

Figure 2. Cold dispase II digest improves the viability and yield of highly pure MACS sorted CD45$^-$CD31$^-$EpCAM$^+$ cells. (**a**) Representative gating strategy for hot and cold digestion following debris exclusion (FSC/SSC) and singlets (FSC-H/FSC-A) for analysis of viability of CD45$^-$CD31$^-$EpCAM$^+$ AECs. (**b**) Comparison of frequency of viable FACS-sorted CD45$^-$CD31$^-$EpCAM$^+$ through live/dead near-IR fixable dye. Unpaired t-test (n=21-33), median ± min/max. (**c**) Comparison of cell yield between the digest methods after CD45, CD31 MACS depletion and EpCAM$^+$ MACS selection. Quantification using haemocytometer and trypan blue live/dead exclusion. Unpaired t-test (n=8), median ± min/max. (**d**) Evaluation of cell suspension purity after MACS sorting CD45$^-$CD31$^-$EpCAM$^+$ cells using flow cytometry. Each data point corresponds to a single murine lung. (**e**) Validating the CD45$^-$CD31$^-$EpCAM$^+$ cells identity. CD45$^-$CD31$^-$EpCAM$^+$ cells also express CD49f and CD24. Presented gating followed debris exclusion (FSC/SSC), singlets gating (FSC-H/FSC-A), live cells gating (LIVE/DEAD fixable near-IR/FSC-H), CD45 and CD31 exclusion (CD45/CD31) and EpCAM$^+$ gating (EpCAM/FSC-H).

3.3 Following Cold Digestion and MACS Sorting, More Basal Cell Colonies Proliferate In Vitro

To investigate if the observed increase in AEC viability with cold digestion translated to greater recovery of airway basal cells in vitro, we seeded 2x10^5 MACS sorted CD45$^-$CD31$^-$EpCAM$^+$ cells (98% purity) from hot or cold lung digestions into 24-well plates (workflow indicated in Figure 3a). Cells were cultured for seven days in Promocell airway epithelial media supplemented with differentiation inhibitors and a Wnt pathway activator*[31–33]*. After seven days the cells were fixed and stained for markers of epithelial (E-cadherin) and basal cells (KRT5 and p63) *[1,34]*. Then 25% of the surface area of each 24-well plate was imaged and the number of basal cell colonies was quantified, as well as the total surface area of KRT5$^+$ basal cell colonies per well (Figure 3b). KRT5$^+$ colony morphology was visualized using phase-contrast microscopy (Figure 3c). On average there were 21 ± 2.97 basal cell colonies after hot digestion and 34 ± 2.98 colonies after cold digestion per 52.6mm^2, which equals to a 1.62-fold increase in colony counts. When we assessed the total surface area of KRT5$^+$ colonies between the two digestion methods, we found a 2.3-fold increase in colony surface area with an average surface area occupied by KRT5$^+$ colonies of 0.66 ± 0.13mm^2 after cold digestions compared to 0.30 ± 0.07mm^2 after hot digestions (Figure 3d). Furthermore, there were very few E-cadherin negative non-epithelial cells in cultures irrespective of the digestion method employed, suggesting that the combination of cold digestion, MACS sorting, and appropriate media allows for propagating highly pure AECs.

Preprints (www.preprints.org) | NOT PEER-REVIEWED | Posted: 12 July 2023 doi:10.20944/preprints202307.0769.v1

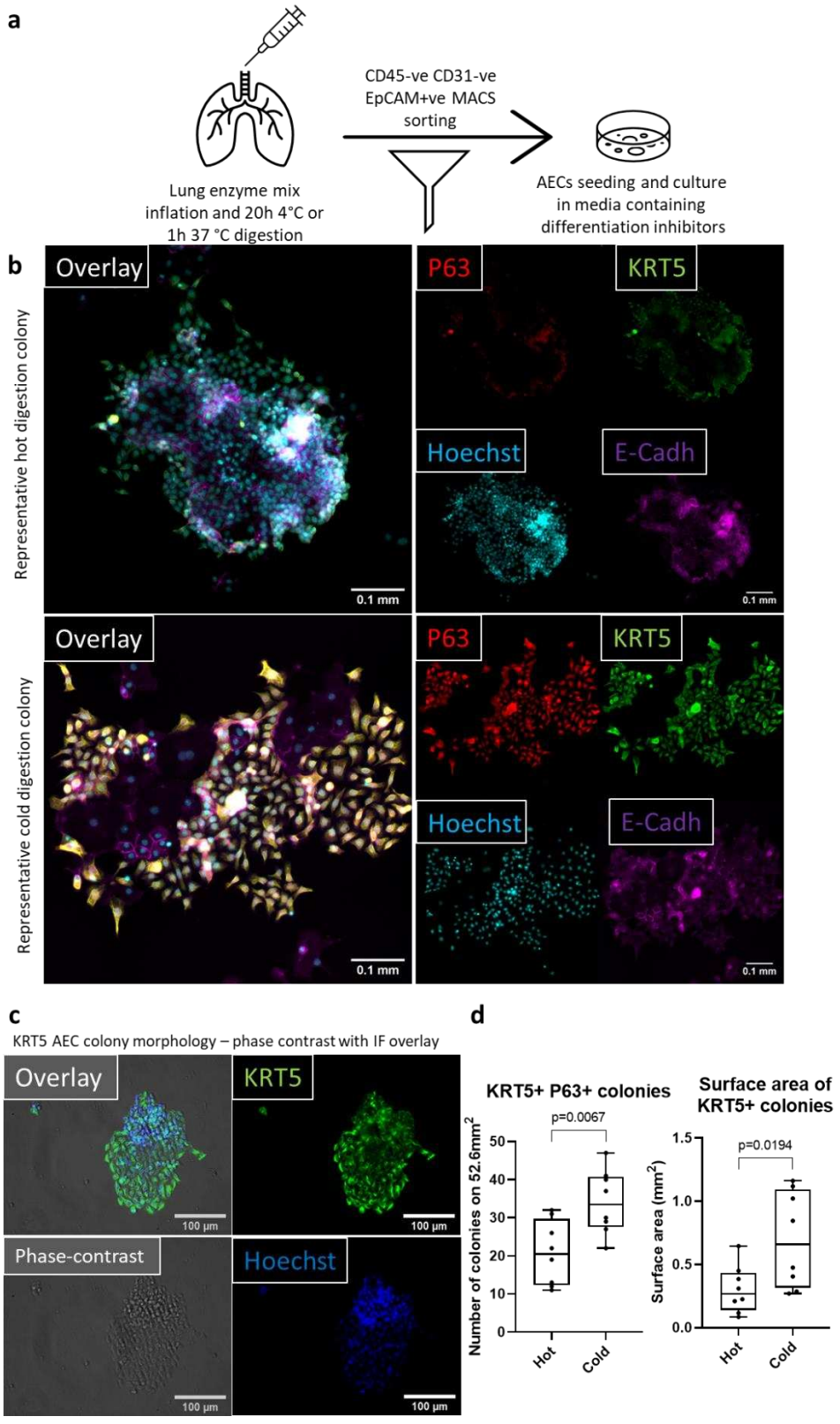

Figure 3. Improved AECs viability translates to a better performance in *in vitro* culture. Cold digestion culture yields a greater number of basal cell colonies, which occupy a larger area. (**a**) Workflow diagram representing the steps involved in digesting the murine lungs and MACS sorting AECs for in vitro culture. (**b**) Representative immunofluorescent micrographs (cold digestion) of P63 (red), KRT5 (green), Hoechst (blue) and E-Cadherin (magenta) used for quantification of the number of P63 and KRT5 double positive colonies. Top scale bar, 2mm. Bottom scale bar (crop), 0.1mm. 25% of each 24-WP well imaged, which

 doi:10.20944/preprints202307.0769.v1

equals to area of 52.6mm^2. Each well was imaged starting from the centre. (**c**) 20x magnification phase-contrast (grey) image overlayed with immunofluorescent KRT5 (green) and Hoechst (blue) images to present morphology of KRT5+ cells. Scale bar (white bar), 100μm (**d**) Quantification of the number (left) and surface area (right) of basal AECs colonies. Colony was defined as ten E-cadh/P63/KRT5+ve cells in immediate vicinity. Colony numbers were quantified based on E-cadh/P63/KRT5+ cells, while colony surface was quantified using only KRT5 pixels. Unpaired t-test (n=8), median ± min/max. Each data point is a single well cultured from MACS sorted CD45- CD31- EpCAM+ isolated from a single murine lung.

4. Discussion

Here, we demonstrate that by changing standard dispase II/DNase I digestion conditions from 1h 37°C to 20h 4°C we are able to obtain significantly greater numbers of lung structural cells, including AECs. This, together with the observation that a higher proportion of AECs are viable after cold digestion suggests that there is a potential to employ cold dispase II lung digestion for establishing primary murine AECs cultures *in vitro*. Indeed, in combination with MACS CD45$^-$CD31$^-$EpCAM$^+$ AEC sorting, we demonstrate that culture of AECs after cold dispase digestion results in a significantly greater number of basal AEC colonies with a larger surface area than after hot digestion. Although establishing culture protocols for murine lung basal AECs was not within the scope of this project, by altering media composition we were able to culture CD45-CD31EpCAM+ MACS sorted cells for up to 14 days over two passages (Supplementary Figure 3a). Additionally, all cells did express KRT5 at the end of passaging period (Supplementary Figure 3b).

These improvements overcome the need for pooled AEC isolates from several mice [24,30,35] and allow for a more comprehensive analysis of AECs from individual animals. This will contribute to the principles of replacement, reduction, and refinement (3R) [36] by reducing the number of mice used in AEC research. However, the greater yield and viability are not the only benefits. The fact that after cold digestion the number of isolated AECs increases substantially suggests that overall AEC populations, including rare and difficult-to-isolate populations, may be better represented in comparison to hot digestion. While further analysis is required to formally confirm our prediction, this is likely to have major implications for researchers studying transcriptomics, epigenomics or proteomics of isolated murine AECs, especially at single cell level. It is possible that by employing hot digestion, only the mostly easily dislodged and/or the most robust AECs are released and survive, potentially skewing analysis. When comparing the abundance of cell types in the murine lung between single-cell RNA sequencing (scRNAseq) and single-nuclear RNA sequencing (snRNAseq), it was reported that scRNAseq under-represents epithelial population in comparison to snRNAseq. Indeed, neuroendocrine and basal cells were exclusively seen in the snRNAseq data sets, while type-1 pneumocytes, club cells and ciliated cells were much better represented in scRNAseq. This might be explained by the fact that single-cell suspension for the scRNAseq is obtained through enzymatic digestion, while nuclei for snRNAseq are isolated through physical dissociation of the tissue [37]. This observation therefore suggests that, in order to isolate representative live epithelial populations through enzymatic digestion, further optimisation is required.

A method commonly used in combination with AEC isolation from tracheas is the removal of fibroblasts by adherence, which requires an additional incubation step, which may further contribute to deteriorating the viability of AECs [7,38]. Alternatively, FACS is used to sort AECs from lung digestions, however, FACS may not only be detrimental to viability of sorted cells, but also limits the number of samples that can be sorted in parallel [39,40]. Here we suggest combining the cold digestion approach with a two-step MACS sorting of CD45$^-$CD31$^-$EpCAM$^+$ cells, which allows for parallel sorting of multiple highly pure samples from larger animal cohorts.

Historically, researchers used tracheas to isolate basal cells from murine airways[4,7], however, the workflow presented here allows for isolation of sufficient numbers of viable basal cells from the lung (without trachea) for successful *in vitro* cultures. These lung-derived basal cells may well differ from their tracheal counterparts, as has been found in human airways, and culture models based on lung derived basal cells may allow a closer representation of the pulmonary epithelium.

In conclusion, we have established a workflow which is based on cold dispase II/DNase I digestion that allows for recovery of a greater number of highly viable AECs, which together with MACS sorting enables quick and parallel isolation of highly pure AEC populations from murine lungs that are suitable for *in vitro* culture.

Supplementary Materials: The following supporting information can be downloaded at the website of this paper posted on Preprints.org. Supplementary figure 1: Cold digestion with dispase II does not remove MHC-I, MHC-II or CD24 from the surface of CD45-CD31-EpCAM+ cells. Supplementary figure 2: Digestion type does not affect cellular oxidative stress based on LDHa (lactate dehydrogenase) levels. Supplementary figure 3: Murine AECs can be passaged (P0-2) following cold digestion and CD45-CD31-EpCAM+ MACS sorting.

Author Contributions: PPJ: Conceptualization, Formal analysis, Investigation, Writing - original draft, Writing - review and editing. CC, HJM: Conceptualization, Formal analysis, Investigation, Writing - review and editing; PS, GPW: Formal analysis, Writing - review and editing. JS: Conceptualization, Data curation, Supervision, Funding acquisition, Writing - original draft, Project administration, Writing - review and editing.

Funding: This research was funded by British Lung Foundation and the Breathing Together Consortium, grant number "PHD16-19 BUSH" and Horserace Betting Levy Board, grant number "VET/2020 -1 EPDF 7".

Institutional Review Board Statement: The animal study protocol was approved by the University of Edinburgh Animal Welfare and Ethical Review Board. UK Home Office project license to JS, number P4871232F.

Informed Consent Statement: Not applicable.

Data Availability Statement: The data underlying this article will be shared upon reasonable request.

Acknowledgments: PPJ and JS thank the British Lung Foundation and the Breathing Together Consortium for support. CC was also supported by a veterinary postdoctoral research fellowship funded by the Horserace Betting Levy Board (VET/2020 -1 EPDF 7). We gratefully acknowledge assistance and expertise from the Flow Core Facility and Microscopy Core Facility at the University of Edinburgh.

Conflicts of Interest: The authors declare no conflict of interest. The funders had no role in the design of the study; in the collection, analyses, or interpretation of data; in the writing of the manuscript; or in the decision to publish the results.

References

1. Rock, J.R.; Randell, S.H.; Hogan, B.L.M. Airway Basal Stem Cells: A Perspective on Their Roles in Epithelial Homeostasis and Remodeling. *Dis Model Mech* 2010, *3*, 545–556, doi:10.1242/dmm.006031.
2. Vaughan, A.E.; Brumwell, A.N.; Xi, Y.; Gotts, J.; Brownfield, D.G.; Treutlein, B.; Tan, K.; Tan, V.; Liu, F.; Looney, M.R.; et al. Lineage-Negative Progenitors Mobilize to Regenerate Lung Epithelium after Major Injury. *Nature* 2015, *517*, 621–625, doi:10.1038/nature14112.
3. Zuo, W.; Zhang, T.; Wu, D.Z.; Guan, S.P.; Liew, A.-A.; Yamamoto, Y.; Wang, X.; Lim, S.J.; Vincent, M.; Lessard, M.; et al. P63+Krt5+ Distal Airway Stem Cells Are Essential for Lung Regeneration. *Nature* 2015, *517*, 616–620, doi:10.1038/nature13903.
4. Eenjes, E.; Mertens, T.C.J.; Kempen, M.J.B.; Wijck, Y. van; Taube, C.; Rottier, R.J.; Hiemstra, P.S. A Novel Method for Expansion and Differentiation of Mouse Tracheal Epithelial Cells in Culture. *Sci Rep-uk* 2018, *8*, 7349, doi:10.1038/s41598-018-25799-6.
5. McQualter, J.L.; Yuen, K.; Williams, B.; Bertoncello, I. Evidence of an Epithelial Stem/Progenitor Cell Hierarchy in the Adult Mouse Lung. *Proc National Acad Sci* 2010, *107*, 1414–1419, doi:10.1073/pnas.0909207107.
6. Jiang, D.; Schaefer, N.; Chu, H.W. Lung Innate Immunity and Inflammation, Methods and Protocols. *Methods Mol Biology* 2018, *1809*, 91–109, doi:10.1007/978-1-4939-8570-8_8.
7. You, Y.; Richer, E.J.; Huang, T.; Brody, S.L. Growth and Differentiation of Mouse Tracheal Epithelial Cells: Selection of a Proliferative Population. *Am J Physiol-lung C* 2002, *283*, L1315–L1321, doi:10.1152/ajplung.00169.2002.
8. Davidson, D.J.; Kilanowski, F.M.; Randell, S.H.; Sheppard, D.N.; Dorin, J.R. A Primary Culture Model of Differentiated Murine Tracheal Epithelium. *Am J Physiol-lung C* 2000, *279*, L766–L778, doi:10.1152/ajplung.2000.279.4.l766.
9. Broadbent, L.; Villenave, R.; Guo-Parke, H.; Douglas, I.; Shields, M.D.; Power, U.F. Human Respiratory Syncytial Virus, Methods and Protocols. *Methods Mol Biology* 2016, *1442*, 119–139, doi:10.1007/978-1-4939-3687-8_9.
10. Vazquez-Armendariz, A.I.; Seeger, W.; Herold, S.; Agha, E.E. Protocol for the Generation of Murine Bronchiolospheres. *Star Protoc* 2021, *2*, 100594, doi:10.1016/j.xpro.2021.100594.

11. Kong, J.; Wen, S.; Cao, W.; Yue, P.; Xu, X.; Zhang, Y.; Luo, L.; Chen, T.; Li, L.; Wang, F.; et al. Lung Organoids, Useful Tools for Investigating Epithelial Repair after Lung Injury. *Stem Cell Res Ther* 2021, *12*, 95, doi:10.1186/s13287-021-02172-5.
12. Teixeira, V.H.; Nadarajan, P.; Graham, T.A.; Pipinikas, C.P.; Brown, J.M.; Falzon, M.; Nye, E.; Poulsom, R.; Lawrence, D.; Wright, N.A.; et al. Stochastic Homeostasis in Human Airway Epithelium Is Achieved by Neutral Competition of Basal Cell Progenitors. *Elife* 2013, *2*, e00966, doi:10.7554/elife.00966.
13. Weitnauer, M.; Mijošek, V.; Dalpke, A.H. Control of Local Immunity by Airway Epithelial Cells. *Mucosal Immunol* 2016, *9*, 287–298, doi:10.1038/mi.2015.126.
14. Crosby, L.M.; Waters, C.M. Epithelial Repair Mechanisms in the Lung. *Am J Physiol-lung C* 2010, *298*, L715–L731, doi:10.1152/ajplung.00361.2009.
15. Heijink, I.H.; Kuchibhotla, V.; Roffel, M.P.; Maes, T.; Knight, D.A.; Sayers, I.; Nawijn, M.C. Epithelial Cell Dysfunction, a Major Driver of Asthma Development. *Allergy* 2020, *75*, 1902–1917, doi:10.1111/all.14421.
16. Gao, W.; Li, L.; Wang, Y.; Zhang, S.; Adcock, I.M.; Barnes, P.J.; Huang, M.; Yao, X. Bronchial Epithelial Cells in COPD. *Respirology* 2015, *20*, 722–729, doi:10.1111/resp.12542.
17. Chakraborty, A.; Mastalerz, M.; Ansari, M.; Schiller, H.B.; Staab-Weijnitz, C.A. Emerging Roles of Airway Epithelial Cells in Idiopathic Pulmonary Fibrosis. *Cells* 2022, *11*, 1050, doi:10.3390/cells11061050.
18. Quantius, J.; Schmoldt, C.; Vazquez-Armendariz, A.I.; Becker, C.; Agha, E.E.; Wilhelm, J.; Morty, R.E.; Vadász, I.; Mayer, K.; Gattenloehner, S.; et al. Influenza Virus Infects Epithelial Stem/Progenitor Cells of the Distal Lung: Impact on Fgfr2b-Driven Epithelial Repair. *Plos Pathog* 2016, *12*, e1005544, doi:10.1371/journal.ppat.1005544.
19. Raoust, E.; Balloy, V.; Garcia-Verdugo, I.; Touqui, L.; Ramphal, R.; Chignard, M. Pseudomonas Aeruginosa LPS or Flagellin Are Sufficient to Activate TLR-Dependent Signaling in Murine Alveolar Macrophages and Airway Epithelial Cells. *Plos One* 2009, *4*, e7259, doi:10.1371/journal.pone.0007259.
20. Naikawadi, R.P.; Disayabutr, S.; Mallavia, B.; Donne, M.L.; Green, G.; La, J.L.; Rock, J.R.; Looney, M.R.; Wolters, P.J. Telomere Dysfunction in Alveolar Epithelial Cells Causes Lung Remodeling and Fibrosis. *Jci Insight* 2016, *1*, e86704, doi:10.1172/jci.insight.86704.
21. Corporation, W.B. Worthington Enzyme Manual Available online: https://www.worthington-biochem.com/tissuedissociation/Lung.html.
22. Supp, D.M.; Hahn, J.M.; Combs, K.A.; McFarland, K.L.; Powell, H.M. Isolation and Feeder-Free Primary Culture of Four Cell Types from a Single Human Skin Sample. *Star Protoc* 2022, *3*, 101172, doi:10.1016/j.xpro.2022.101172.
23. Volovitz, I.; Shapira, N.; Ezer, H.; Gafni, A.; Lustgarten, M.; Alter, T.; Ben-Horin, I.; Barzilai, O.; Shahar, T.; Kanner, A.; et al. A Non-Aggressive, Highly Efficient, Enzymatic Method for Dissociation of Human Brain-Tumors and Brain-Tissues to Viable Single-Cells. *Bmc Neurosci* 2016, *17*, 30, doi:10.1186/s12868-016-0262-y.
24. You, Y.; Richer, E.J.; Huang, T.; Brody, S.L. Growth and Differentiation of Mouse Tracheal Epithelial Cells: Selection of a Proliferative Population. *Am J Physiol-lung C* 2002, *283*, L1315–L1321, doi:10.1152/ajplung.00169.2002.
25. Autengruber, A.; Gereke, M.; Hansen, G.; Hennig, C.; Bruder, D. Impact of Enzymatic Tissue Disintegration on the Level of Surface Molecule Expression and Immune Cell Function. *European J Microbiol Immunol* 2012, *2*, 112–120, doi:10.1556/eujmi.2.2012.2.3.
26. Mokwatsi, G.G.; Schutte, A.E.; Kruger, R. A Biomarker of Tissue Damage, Lactate Dehydrogenase, Is Associated with Fibulin-1 and Oxidative Stress in Blacks: The SAfrEIC Study. *Biomarkers* 2015, *21*, 48–55, doi:10.3109/1354750x.2015.1118532.
27. Li, X.; Rossen, N.; Sinn, P.L.; Hornick, A.L.; Steines, B.R.; Karp, P.H.; Ernst, S.E.; Adam, R.J.; Moninger, T.O.; Levasseur, D.N.; et al. Integrin A6β4 Identifies Human Distal Lung Epithelial Progenitor Cells with Potential as a Cell-Based Therapy for Cystic Fibrosis Lung Disease. *Plos One* 2013, *8*, e83624, doi:10.1371/journal.pone.0083624.
28. Chernaya, O.; Shinin, V.; Liu, Y.; Minshall, R.D. Behavioral Heterogeneity of Adult Mouse Lung Epithelial Progenitor Cells. *Stem Cells Dev* 2014, *23*, 2744–2757, doi:10.1089/scd.2013.0631.
29. Nakano, H.; Nakano, K.; Cook, D.N. Type 2 Immunity, Methods and Protocols. *Methods Mol Biology* 2018, *1799*, 59–69, doi:10.1007/978-1-4939-7896-0_6.
30. Chen, H.; Matsumoto, K.; Brockway, B.L.; Rackley, C.R.; Liang, J.; Lee, J.; Jiang, D.; Noble, P.W.; Randell, S.H.; Kim, C.F.; et al. Airway Epithelial Progenitors Are Region Specific and Show Differential Responses to Bleomycin-Induced Lung Injury. *Stem Cells* 2012, *30*, 1948–1960, doi:10.1002/stem.1150.
31. Nichane, M.; Javed, A.; Sivakamasundari, V.; Ganesan, M.; Ang, L.T.; Kraus, P.; Lufkin, T.; Loh, K.M.; Lim, B. Isolation and 3D Expansion of Multipotent Sox9 + Mouse Lung Progenitors. *Nat Methods* 2017, *14*, 1205–1212, doi:10.1038/nmeth.4498.
32. Eenjes, E.; Mertens, T.C.J.; Kempen, M.J.B.-V.; Wijck, Y.V.; Taube, C.; Rottier, R.J.; Hiemstra, P.S. A Novel Method for Expansion and Differentiation of Mouse Tracheal Epithelial Cells in Culture. *Sci Rep-uk* 2018, *8*, 1–12, doi:10.1038/s41598-018-25799-6.

33. Levardon, H.; Yonker, L.; Hurley, B.; Mou, H. Expansion of Airway Basal Cells and Generation of Polarized Epithelium. *Bio-protocol* 2018, *8*, doi:10.21769/bioprotoc.2877.
34. Zuo, W.; Zhang, T.; Wu, D.Z.A.; Guan, S.P.; Liew, A.A.; Yamamoto, Y.; Wang, X.; Lim, S.J.; Vincent, M.; Lessard, M.; et al. P63 + Krt5 + Distal Airway Stem Cells Are Essential for Lung Regeneration. *Nature* 2015, *517*, 616–620, doi:10.1038/nature13903.
35. Lam, H.C.; Choi, A.M.K.; Ryter, S.W. Isolation of Mouse Respiratory Epithelial Cells and Exposure to Experimental Cigarette Smoke at Air Liquid Interface. *J Vis Exp* 2011, doi:10.3791/2513.
36. Prescott, M.J.; Lidster, K. Improving Quality of Science through Better Animal Welfare: The NC3Rs Strategy. *Lab Animal* 2017, *46*, 152–156, doi:10.1038/laban.1217.
37. Koenitzer, J.R.; Wu, H.; Atkinson, J.J.; Brody, S.L.; Humphreys, B.D. Single-Nucleus RNA-Sequencing Profiling of Mouse Lung. Reduced Dissociation Bias and Improved Rare Cell-Type Detection Compared with Single-Cell RNA Sequencing. *Am J Resp Cell Mol* 2020, *63*, 739–747, doi:10.1165/rcmb.2020-0095ma.
38. Lee, D.F.; Salguero, F.J.; Grainger, D.; Francis, R.J.; MacLellan-Gibson, K.; Chambers, M.A. Isolation and Characterisation of Alveolar Type II Pneumocytes from Adult Bovine Lung. *Sci Rep-uk* 2018, *8*, 11927, doi:10.1038/s41598-018-30234-x.
39. Pan, J.; Wan, J. Methodological Comparison of FACS and MACS Isolation of Enriched Microglia and Astrocytes from Mouse Brain. *J Immunol Methods* 2020, *486*, 112834, doi:10.1016/j.jim.2020.112834.
40. Sutermaster, B.A.; Darling, E.M. Considerations for High-Yield, High-Throughput Cell Enrichment: Fluorescence versus Magnetic Sorting. *Sci Rep-uk* 2019, *9*, 227, doi:10.1038/s41598-018-36698-1.